Role of screened exact exchange in accurately describing properties of transition metal oxides: Modeling defects in $LaAlO_3$

Fedwa El-Mellouhi,[1,2,*] Edward N. Brothers,[1,†] Melissa J. Lucero,[3] and Gustavo E. Scuseria[3,4,5]
[1]*Chemistry Department, Texas A&M at Qatar, Texas A&M Engineering Building, Education City, Doha, Qatar*
[2]*Physics Department, Texas A&M at Qatar, Texas A&M Engineering Building, Education City, Doha, Qatar*
[3]*Department of Chemistry, Rice University, Houston, Texas 77005-1892, USA*
[4]*Department of Physics and Astronomy, Rice University, Houston, Texas 77005-1892, USA*
[5]*Chemistry Department, Faculty of Science, King Abdulaziz University, Jeddah 21589, Saudi Arabia*
(Received 4 August 2013; revised manuscript received 29 September 2013; published 3 December 2013)

The properties of many intrinsic defects in the wide-band-gap semiconductor $LaAlO_3$ are studied using the screened hybrid functional of Heyd, Scuseria, and Ernzerhof (HSE) [J. Chem. Phys. **118**, 8207 (2003)]. As in pristine structures, exact exchange included in the screened hybrid functional alleviates the band-gap underestimation problem, which is common to semilocal functionals; this allows accurate prediction of defect properties. We propose correction-free defect energy levels for bulk $LaAlO_3$ computed using HSE that might serve as a guide in the interpretation of photoluminescence experiments.

DOI: 10.1103/PhysRevB.88.214102 PACS number(s): 71.15.Mb, 71.15.Ap

Defects in $LaAlO_3$ have been studied extensively both experimentally[1] and using computational approaches,[2,3] contributing to our understanding of the interplay between various defects in this material. Photoluminescence (PL) spectroscopy using subband-gap excitation was recently used to detect the ground-state defect states within the band gap of $LaAlO_3$ single crystals.[1] In standard photoluminescence, electrons are pumped to the conduction band, then a photon is emitted upon relaxation from the conduction band to various ground-state defect levels. The resulting PL peaks are then associated with defect levels inside the gap. In subband-gap excitation, the photon energy is tuned to selectively probe certain defect levels, revealing more detailed features. This experiment identified three distinct PL peaks, each showing doublet splitting, that were localized 2 eV below the conduction-band minimum (CBM). Defect levels calculated[2] using the the generalized gradient approximation density functional of Perdew, Burke, and Ernzerhof (PBE)[4,5] and corrected with the "scissor operator" were used as a guideline to partially match the PL peaks. This approach is less than completely satisfying, however, as (for example) the La_{Al} defect level, post-correction, is located 1 eV below the CBM; this contradicts recent experimental results. A more accurate theoretical description is thus much needed, especially given the problems of band-gap underestimation (endemic to semilocal functionals),[6] which is fatal for defect calculations, and questions about the overall appropriateness of the "scissor operator." Put more simply, the typical theoretical methods which can be used for modeling these sorts of materials are insufficiently accurate for explaining the effects in question.

Defects in $LaAlO_3$ have been subject to other very recent theoretical calculations:[3,7] Vacancy defect energetics in rhombohedral and cubic bulk $LaAlO_3$ have been computed using PBE in Ref. 3, where it was found that the defect formation behavior in both phases was very similar. That work also included finite-size scaling using supercells up to 480 atoms, suggesting that the cell-size dependencies in modeling neutral vacancies are almost negligible. (This makes their formation energies almost independent from the supercell size.) However, it should be noted that formation energies were modified using a band-gap correction scheme[3] to overcome the well-known band-gap underestimation problem of semilocal functionals. For this reason, interest has emerged in using modern (and demonstrably more accurate)[8] screened hybrid functionals to model these defects. While some recent efforts have been published in this direction,[7,9] a complete picture of all possible defect levels using modern hybrid functionals is not available.

In the present work, we apply the screened hybrid functional of Heyd-Scuseria-Ernzerhof (HSE) to a wide array of neutral defect types in $LaAlO_3$, thus complementing previous HSE efforts[7] that treated only the oxygen vacancies. This work is motivated by HSE's agreement with experiment for the calculation of many of the electronic, structural, and elastic properties in cubic $LaAlO_3$.[10] HSE is expected to give point-defect formation energies and energy levels in close agreement with experiment as its direct and indirect band gaps[10] as well as valence-band widths (VBWs)[11] are in excellent agreement with experiment (see Table I); this can be contrasted with the PBE results, which have been previously used to study point defects in $LaAlO_3$.[2,3] It is worth noting that HSE06 gives an excellent agreement with the results of the global hybrid PBE0 for the case of the oxygen vacancy in $SrTiO_3$.[12] This suggests that hybrid functionals belonging to the 25% HF exchange family such as PBE0 and HSE06 would yield a very similar location for the defect level and the splitting of the conduction-band minimum in the $LaAlO_3$ case as well.

Here we restrict our study to neutral defects to avoid introducing errors due to spurious electrostatic interactions, and the corrections associated with it. Nevertheless, performing HSE calculations with the high-numerical-accuracy settings detailed below remains quite expensive, thus precluding the use of the largest supercells. This is acceptable, however, as finite-size scaling and previous investigations[3,7] using larger supercells have shown that the neutral defects considered here suffer least from finite-size effects. Consequently, despite the limited number of atoms that can be treated with HSE, this approach promises increased physical accuracy compared to the less expensive semilocal functionals.

TABLE I. Comparison of calculated fundamental electronic properties of bulk cubic $LaAlO_3$ from this work and previous studies. VBW stands for the valence-band width. Calculated enthalpies of formation in eV/atom for idealized materials with phases containing La, Al, and O are compared to previous PBE calculations[2] and experiment.

	This Work		Previous Work	
	HSE	PBE	PBE	Expt.
Direct gap (eV)	5.0	3.54		
Indirect gap (eV)	4.74	3.26	3.1[e]	
VBW (R→R)(eV)	8.00	7.50		
$\Delta H^f_{Al_2O_3}$	3.82	3.6	3.30[a]	3.47[b]
$\Delta H^f_{La_2O_3}$	4.24	4.00	3.71[a]	3.71[c]
$\Delta H^f_{LaAlO_3}$	3.78	4.21	3.60[a]	3.45[d]

[a]Reference 2.
[b]Reference 19.
[c]Reference 20.
[d]Reference 21.
[e]Reference 9.

All calculations presented in this paper were performed using the development version of the GAUSSIAN suite of programs,[13] with the periodic boundary condition (PBC)[14] code used throughout. The Def2-[15] series of Gaussian basis sets were optimized following our procedure described in Ref. 16 for bulk $LaAlO_3$. As in Ref. 16, we use the notation SZVP to differentiate these optimized PBC basis sets from the molecular Def2-SZVP basis sets. The functionals applied in this work include PBE[4,5] and HSE.[17]

The use of HSE imposes limitations on the size of the supercell that can be efficiently computed and fully relaxed, so a LAO supercell of $2 \times 2 \times 2$ replica of the 5 atoms cubic unit cell (40 atoms) was used with a dense k-point mesh of $6 \times 6 \times 6$, including the Γ point. Also, we modeled a larger supercell of $2 \times 3 \times 3$ (90 atoms), with the same density of k points, in order to discuss the importance of defect self-interactions and the effect of varying the defect concentration on the electronic properties of LAO.

Most numerical settings in GAUSSIAN were left at the default values, e.g., geometry optimization settings, integral cutoffs, k-point meshes, and SCF convergence thresholds. Unless otherwise noted, crystal structures used in the chemical potential calculations on La, Al, Al_2O_3, and La_2O_3 were downloaded as crystallographic information files (CIF) from the inorganic crystal structure database (ICSD),[18] and then fully relaxed/optimized. Isolated, neutral vacancies were introduced to the crystal structure of cubic LAO by removing one atom of either O, La, or Al, while La and Al antisites occupied the crystalline position. All structures containing the above defects were then fully relaxed using HSE06. In order to avoid imposing a certain oxygen interstitial position, the oxygen atom was inserted far from the well-known interstitial sites followed by relaxation to the nearest minimum. At this point, we cannot be completely sure whether or not the configuration we obtained has the lowest formation energy; only a full energy landscape exploration method can reveal that.

The calculations of neutral defect formation energies used the formalism of Zhang and Northrup,[22] namely, the equation

$$E_f = E_T - [E_T(\text{perfect}) - n_{\text{La}}\mu_{\text{La}} - n_{\text{Al}}\mu_{\text{Al}} - n_O\mu_O], \quad (1)$$

where E_T and E_T(perfect) are the calculated total energies of the supercells containing the point defect and the perfect bulk host materials, respectively. The number of each element removed from the perfect supercell is represented by n_x, while μ_x corresponds to the atomic chemical potentials in an $LaAlO_3$ crystal. Assuming that $LaAlO_3$ is always stable, the chemical potentials of the these elements can vary in the following correlation:

$$\mu_{\text{La}} + \mu_{\text{Al}} + 3\mu_O = \mu^{\text{bulk}}_{\text{LaAlO}_3}. \quad (2)$$

Obviously, atomic chemical potentials are determined by the sample composition and cannot be ascertained exactly. However, they can be varied to cover the whole phase diagram of LAO splitting into Al_2O_3 and La_2O_3 bulk phases. Hence the calculated formation energies for the neutral point defects vary according to equilibrium positions such as "O-rich" and "O-poor" conditions.

The calculated enthalpies of formation in idealized materials (nonrelaxed structures) for phases containing La, Al, and O are summarized in Table I and are compared to previous calculations[2] and experiments. As a general trend, the formation enthalpies computed with HSE are close to the results from semilocal functionals such as PBE (this work), although the HSE values are slightly higher. The only exception is $LaAlO_3$, where PBE tends to overestimate the formation enthalpies and exceed the HSE value.

The formation energies of defects in LAO as a function of its composition are plotted in Fig. 1.[23] Under oxidizing conditions (points A and B), we identify the oxygen interstitial (O_I) as having the lowest formation energy; this is contrary to previous PBE results[2] which predicted O_I to be less stable than V_{La} and other vacancy complexes. It is worth noting that we introduced the oxygen atom at a random position in the supercell avoiding well-known interstitial sites followed by a full relaxation of the system. The resulting configuration consists of a 110 split interstitial (dumbbell) with an O-O bond of 1.38 Å. Since Luo *et al.*[2] did not report their interstitial

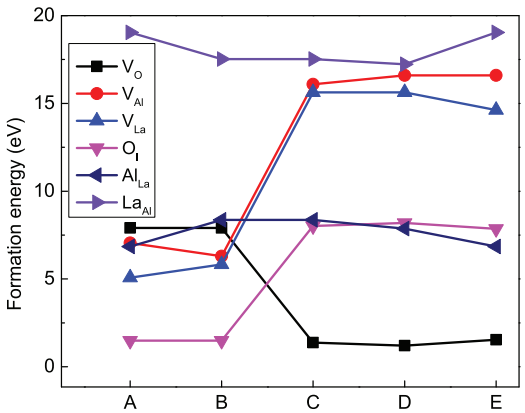

FIG. 1. (Color online) Defect formation energies of isolated defects in cubic LAO computed using HSE at each equilibrium point based upon the phase diagram in Ref. 2.

configuration, we could assume that our differences arise from different interstitial sites considered rather than computational differences.

Focusing specifically at point A, V_{La} is the next most stable defect. Our formation energy is about 3 eV higher than previously published results obtained using the PBE functional in rhombohedral and cubic LAO.[2,3] In terms of competition between V_{La} and V_{Al}, we find (using HSE) the same behavior seen using PBE in Refs. 1 and 2. Next in order of stability is V_{Al} and Al_{La} with equal formation energies at point A, followed by V_O, a behavior not reported previously.[2,3]

Moving from point A to point B, the order of increasing stability of defect types remains unchanged, except for Al_{La}, which has become less stable than V_O. We report a formation energy of 8 eV for V_O, which is in excellent agreement with a recently computed HSE value of 8.3 eV in rhombohedral LAO

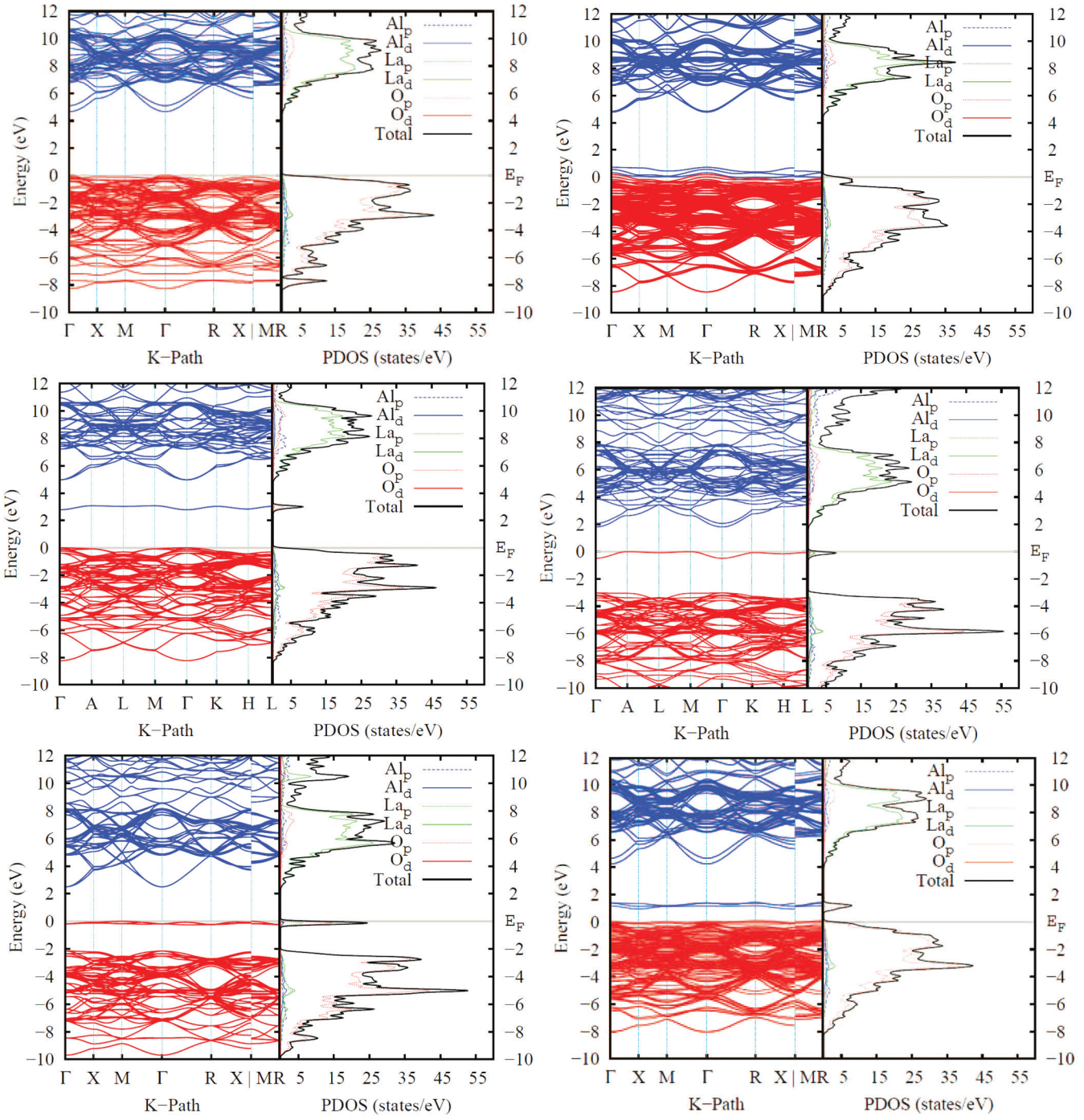

FIG. 2. (Color online) Band structures and PDOS calculated with HSE/SZVP for the $2 \times 2 \times 2$ $LaAlO_3$ supercell containing intrinsic defects. The top figures represent O_I and V_{La} introducing bands with a valence-band character. Al_{La} and V_O (middle row) have bands above the midgap. The bottom row contains La_{Al} and V_{Al} having defect bands below midgap. The Fermi energy E_F is indicated by a solid black line. The red bands indicate the occupied defect bands, while the unoccupied defect bands are shown in blue.

using a supercell of up to 135 atoms;[7] note that in this study other vacancy types and substitutions were not modeled.

Under reducing conditions (points C, D, and E), V_O dominates the spectrum, in qualitative and quantitative agreement with previous uncorrected PBE calculations,[2] having an average formation energy of 1.3 eV. The formation energy of V_O calculated with HSE is lowered by 0.1 eV when the supercell size increases from 40 to 90 atoms. Although not negligible, this remains smaller than the differences reported in the charged states,[2,3,7] which are due to both the strong elastic and electrostatic self-defect interactions. Obviously, calculations using larger fully relaxed supercells are required to determine at what size defect self-interactions (elastic effects) become negligible.

Our results do not agree, however, with the recent formation energies computed by Yamamoto *et al.*[3] who applied a band-gap correction (a 2.48 eV shift) to the PBE formation energies of V_O. Applying the band-gap correction in this case led to the conclusion that Schottky-type vacancy complexes are more stable than V_O. We believe this to be an artifact of the correction they applied.

It should be noted that interstitials such as La_I and Al_I are not addressed in the present study because their neutral charge state was not identified to be stable according to the PBE calculation of Luo *et al.*[2] Also, our formation energy spectrum computed with HSE reveals that they exhibit very high formation energies.

The various defects we will first discuss induce changes to the electronic properties of cubic $LaAlO_3$, introducing defect levels within the band gap and/or lifting the degeneracy of the CBM and VBM as shown in Fig. 2.

The oxygen split interstitial configuration (O_I), which is the most stable under oxidizing conditions, induces a strong distortion to the lattice, which in turn significantly impacts the electronic structure. The CBM splits at the Γ point by 440 meV, while the VBM also splits into three distinct bands. The fully occupied defect band composed of O $2p$ states is located on average at 0.13 eV above the VBM, has valence-band character, and induces a gap of 4.66 eV. V_{La}, the second most stable defect under oxidizing conditions, creates three empty nondegenerate valence bands, dominated by O $2p$ orbitals originating from the O dangling bonds. Both HSE and PBE agree about the nature and the location of these bands. However, our O_I level is shallower than the previously reported PBE results,[2] which is probably due to differences in the interstitial configuration.

Next to be evaluated are defects having in-gap states, namely, Al_{La}, V_O, La_{Al}, and V_{Al}, which show a localized electronic density around the defect region. The Al_{La} antisite defect might play a role under oxidizing conditions due to its relatively low formation energy. With HSE, we find that it induces an empty defect band in the gap at 2.93 eV above the VBM and 2.0 eV below the CBM. This band might become populated upon doping or under excitation, and is dominated by O $2p$ and Al s orbitals [q.v. the partial density of states (PDOS)]. The bulk degeneracy of the VBM and CBM are not affected and remain three- and twofold degenerate, respectively. This is an indication that this defect does not introduce noticeable distortion or octahedral rotation into the lattice, which is further confirmed by a structural analysis. However, using PBE, we find that the Al_{La} defect band is located at 1.22 eV above the VBM and 2 eV below the CBM, which is well below the midgap (1.6 eV). Following a typical band-gap correction procedure, this PBE defect band does not need to be shifted using the scissor operator,[2] which would result in keeping its VB character, which contradicts the HSE results above.

The next defect of interest is V_O, which is arguably the most important defect under reducing conditions and suspected to be systematically introduced during the growth of metal oxide superlattices.[24] After introducing V_O, the supercell shrinks along the y axis, leading to a tetragonal distortion of the lattice with a ratio $a/b = 1.0057$ (a and b being the resulting lattice parameters) and a slight rotation of AlO_6 octahedra. This strongly impacts strongly the electronic structure by splitting the doubly degenerate CBM by 258 meV, while leaving the VBM triply degenerate. Another defect band also appears at 2.77 eV above the VBM from the combination of O $2p$, Al d, La d, and p orbitals. Here again, major differences with previous PBE data emerge: the uncorrected PBE level computed recently by Chen *et al.*[1] was located 2.23 eV above the VBM. Luo *et al.* applied the scissor operator to this defect level, predicting it to lie at about 3.8 eV above the VBM.

Last to be examined is La_{Al}, which in the neutral state would rarely form under either oxidizing or reducing conditions. It

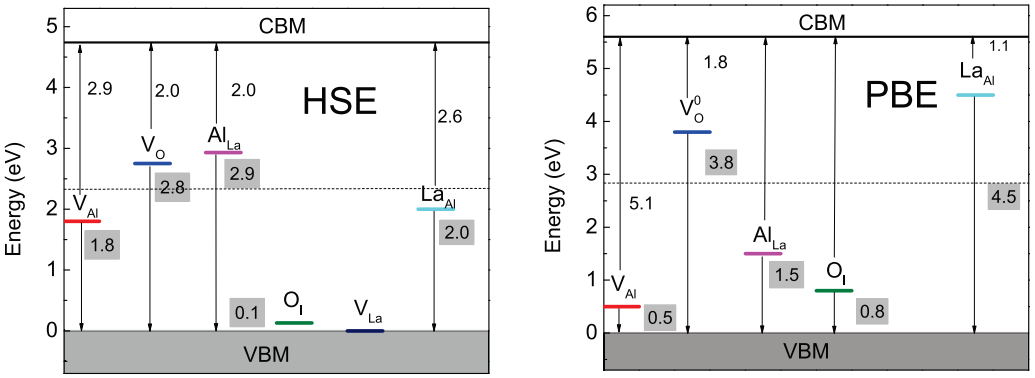

FIG. 3. (Color online) Schematic representation of the average location of the defect bands in the band gap of LAO calculated with HSE/SZVP (left) and PBE from Ref. 2 (right) shifted using a scissor operator. Numbers in gray boxes refer to the location of the defect bands with respect to the valence-band maximum (VBM). The dashed line refers to the midgap.

introduces a fully occupied, triply degenerate defect band located 2.06 eV above the VBM and 2.60 eV below the CBM. However, the PBE defect level is at that method's midgap, lying 1.6 eV from the VBM and CBM. If a scissor operator was to be used, one could argue that this level should be shifted, placing it as close as 1 eV to the CBM (see Fig. 3).

To conclude, there are fundamental differences between our HSE defect level spectrum and the one published earlier using corrected PBE[2] data regarding the nature of the defect bands (see Fig. 3). We believe these differences originate from the criterion used to judge whether the "scissor operator" should be applied. For example, HSE finds that Al_{La} and V_{Al} have defect bands near midgap, thus removing the PBE's prediction of valence-band character, which were reported previously. The same issue leads to significant differences in the conclusions regarding V_O. Overall, our defect levels calculated with HSE lie 2 eV below the CBM (see Fig. 3), which is in better agreement with recent experiment.[1] This HSE defect level spectrum that we propose here is correction free and may be used to interpret experimental photoluminescence data which place defect levels at 3.1, 2.1, and 1.7 eV.[1,25]

This work is supported by the Qatar National Research Fund (QNRF) through the National Priorities Research Program (NPRP Grant No. 08-431-1-076). G.E.S. acknowledges support from The Welch Foundation (Grant No. C-0036). We are grateful to the research computing facilities at Texas A&M University at Qatar for generous allocations of computer resources.

*fadwa.el_mellouhi@qatar.tamu.edu
†ed.brothers@qatar.tamu.edu

[1] J. Q. Chen, X. Wang, Y. H. Lu, A. R. Barman, G. J. You, G. C. Xing, T. C. Sum, S. Dhar, Y. P. Feng, Ariando, Q. H. Xu, and T. Venkatesan, Appl. Phys. Lett. **98**, 041904 (2011).
[2] X. Luo, B. Wang, and Y. Zheng, Phys. Rev. B: Condens. Matter Mater. Phys. **80**, 104115/1 (2009).
[3] T. Yamamoto and T. Mizoguchi, Phys. Rev. B **86**, 094117 (2012).
[4] J. P. Perdew, K. Burke, and M. Ernzerhof, Phys. Rev. Lett. **77**, 3865 (1996).
[5] J. P. Perdew, K. Burke, and M. Ernzerhof, Phys. Rev. Lett. **78**, 1396 (1997).
[6] J. Heyd, J. E. Peralta, G. E. Scuseria, and R. L. Martin, J. Chem. Phys. **123**, 174101 (2005).
[7] C. Mitra, C. Lin, J. Robertson, and A. A. Demkov, Phys. Rev. B **86**, 155105 (2012).
[8] T. M. Henderson, J. Paier, and G. E. Scuseria, Phys. Status Solidi B **248**, 767 (2011).
[9] K. Xiong, J. Robertson, and S. J. Clark, Microelectron. Eng. **85**, 65 (2008).
[10] F. El-Mellouhi, E. N. Brothers, M. J. Lucero, I. W. Bulik, and G. E. Scuseria, Phys. Rev. B **87**, 035107 (2013).
[11] R. Ramprasad, H. Zhu, P. Rinke, and M. Scheffler, Phys. Rev. Lett. **108**, 066404 (2012).
[12] R. Evarestov, E. Blokhin, D. Gryaznov, E. A. Kotomin, R. Merkle, and J. Maier, Phys. Rev. B **85**, 174303 (2012).
[13] Gaussian Development Version, Revision H.07+, M. J. Frisch, G. W. Trucks, H. B. Schlegel, G. E. Scuseria, M. A. Robb, J. R. Cheeseman, G. Scalmani, V. Barone, B. Mennucci, G. A. Petersson, H. Nakatsuji, M. Caricato, X. Li, H. P. Hratchian, A. F. Izmaylov, J. Bloino, G. Zheng, J. L. Sonnenberg, W. Liang, M. Hada, M. Ehara, K. Toyota, R. Fukuda, J. Hasegawa, M. Ishida, T. Nakajima, Y. Honda, O. Kitao, H. Nakai, T. Vreven, J. A. Montgomery, Jr., J. E. Peralta, F. Ogliaro, M. Bearpark, J. J. Heyd, E. Brothers, K. N. Kudin, V. N. Staroverov, T. Keith, R. Kobayashi, J. Normand, K. Raghavachari, A. Rendell, J. C. Burant, S. S. Iyengar, J. Tomasi, M. Cossi, N. Rega, J. M. Millam, M. Klene, J. E. Knox, J. B. Cross, V. Bakken, C. Adamo, J. Jaramillo, R. Gomperts, R. E. Stratmann, O. Yazyev, A. J. Austin, R. Cammi, C. Pomelli, J. W. Ochterski, R. L. Martin, K. Morokuma, V. G. Zakrzewski, G. A. Voth, P. Salvador, J. J. Dannenberg, S. Dapprich, P. V. Parandekar, N. J. Mayhall, A. D. Daniels, O. Farkas, J. B. Foresman, J. V. Ortiz, J. Cioslowski, and D. J. Fox, Gaussian, Inc., Wallingford CT, 2010.
[14] K. N. Kudin and G. E. Scuseria, Phys. Rev. B **61**, 16440 (2000).
[15] F. Weigend and R. Ahlrichs, Phys. Chem. Chem. Phys. **7**, 3297 (2005).
[16] F. El-Mellouhi, E. N. Brothers, M. J. Lucero, and G. E. Scuseria, Phys. Rev. B **84**, 115122 (2011).
[17] T. M. Henderson, A. F. Izmaylov, G. Scalmani, and G. E. Scuseria, J. Chem. Phys. **131**, 044108 (2009), specifically, the HSEh parametrization of HSE06,[26,27] called by the GAUSSIAN keyword HSEh1PBE, with $\omega = 0.11$.
[18] Inorganic Crystallographic Structural Database (ICSD), www.fiz-karlsruhe.de/icsd_web.html, specifically, the ICSD collection ID numbers are bulk La (FCC) 41518, bulk Al (hcp) ($Fm3m$) 43423, Al_2O_3 ($R\bar{3}cH$) 10425, La_2O_3 ($P\bar{3}m1$) 56771.
[19] P. J. Linstrom and W. G. Mallard, eds., NIST Chemistry WebBook, NIST Standard Reference Database Number 69, National Institute of Standards and Technology, Gaithersburg MD, 20899, http://webbook.nist.gov.
[20] E. H. P. Cordfunke and R. J. M. Konings, Thermochim. Acta **375**, 65 (2001).
[21] W. Schnelle, R. Fischer, and E. Gmelin, J. Phys. D: Appl. Phys. **34**, 846 (2001).
[22] S. B. Zhang and J. Northrup, Phys. Rev. Lett. **67**, 2339 (1991).
[23] Point A: $\mu_O = \mu_O(\text{bulk})$, $2\mu_{Al} + 3\mu_O = \mu_{Al_2O_3}(\text{bulk})$ where $\mu_O(\text{bulk})$ corresponds to the chemical potential per atom of O_2 gas.
Point B: $\mu_O = \mu_O(\text{bulk})$, $2\mu_{La} + 3\mu_O = \mu_{La_2O_3}(\text{bulk})$.
Point C: $\mu_{La} = \mu_{La}(\text{bulk})$, $2\mu_{La} + 3\mu_O = \mu_{La_2O_3}(\text{bulk})$.
Point D: $\mu_{La} = \mu_{La}(\text{bulk})$, $\mu_{Al} = \mu_{Al}(\text{bulk})$.
Point E: $\mu_{Al} = \mu_{Al}(\text{bulk})$, $2\mu_{Al} + 3\mu_O = \mu_{Al_2O_3}(\text{bulk})$.
[24] Y. Tian, C. Adamo, D. G. Schlom, and K. S. Burch, Appl. Phys. Lett. **102**, 041906 (2013).
[25] Z. Q. Liu, D. P. Leusink, X. Wang, W. M. Lü, K. Gopinadhan, A. Annadi, Y. L. Zhao, X. H. Huang, S. W. Zeng, Z. Huang, A. Srivastava, S. Dhar, T. Venkatesan, and Ariando, Phys. Rev. Lett. **107**, 146802 (2011).
[26] J. Heyd, G. E. Scuseria, and M. Ernzerhof, J. Chem. Phys. **118**, 8207 (2003).
[27] J. Heyd, G. E. Scuseria, and M. Ernzerhof, J. Chem. Phys. **124**, 219906 (2006).